

Modeling the QSO luminosity and spatial clustering at low redshifts

F. Marulli,¹ D. Crociani,¹ M. Volonteri,² E. Branchini³ and L. Moscardini¹

¹*Dipartimento di Astronomia, Università degli Studi di Bologna, via Ranzani 1, I-40127 Bologna, Italy*

²*Institute of Astronomy, Madingley Road, Cambridge, CB3 0HA, U.K.*

³*Dipartimento di Fisica, Università degli Studi “Roma Tre”, via della Vasca Navale 84, I-00146 Roma, Italy*

12 July 2018

ABSTRACT

We investigate the ability of hierarchical models of QSO formation and evolution to match the observed luminosity, number counts and spatial clustering of quasars at redshift $z < 2$. These models assume that the QSO emission is triggered by galaxy mergers, that the mass of the central black hole correlates with halo properties and that quasars shine at their Eddington luminosity except, perhaps, during the very early stages of evolution. We find that models based on simple analytic approximations successfully reproduce the observed B -band QSO luminosity function at all redshifts, provided that some mechanisms is advocated to quench mass accretion within haloes larger than $\sim 10^{13} M_{\odot}$ that host bright quasars. These models also match the observed strength of QSO clustering at $z \sim 0.8$. At larger redshifts, however, they underpredict the QSO biasing which, instead, is correctly reproduced by semi-analytic models in which the halo merger history and associated BHs are followed by Monte Carlo realizations of the merger hierarchy. We show that the disagreement between the luminosity function predicted by semi-analytic models and observations can be ascribed to the use of B -band data, which are a biased tracer of the quasar population, due to obscuration.

Key words: quasar: general – galaxies: formation – galaxies: active – galaxies: clustering – cosmology: theory – cosmology: observations

1 INTRODUCTION

Observational evidences accumulated over the past few years indicate that the physical properties of supermassive black holes [SBHs, hereafter] residing at the centre of most, if not all, spheroidal galaxies (Richstone et al. 1998), correlate with those of the host galaxy (Magorrian et al. 1998; Ferrarese & Merritt 2000; Gebhardt et al. 2000) and, possibly, of the host dark matter (DM) halo (Ferrarese 2002). Although it is not clear whether the observed correlation between halo and BH masses is genuine or simply reflects the fact that massive haloes preferentially host massive spheroids (Wyithe & Loeb 2005a), the strong connection between the BH properties and the gravitational potential wells that host them suggests a link between the assembly of BHs and the evolution of galaxy spheroids. This co-evolution is expected within the frame of hierarchical models of structure formation, like the popular cold dark matter (CDM) cosmogonies. Since it is generally accepted that the quasar activity is powered by SBHs, several models have been proposed to trace the assembly of SBHs during the hierarchical build-up of their host haloes using numerical, analytic and semi-analytic methods. In this work we focus on the latter two approaches that consist of parameterizing in term of simple analytic models the complex physics of the galaxy formation process, while the evolution of DM haloes can be either followed using numerical

techniques, in the so called semi-analytic approach, or simplified analytic prescriptions, which constitute a full analytic model.

Over the years many different analytic (see, e.g., Efstathiou & Rees 1988; Haehnelt & Rees 1993; Haiman & Loeb 1998; Percival & Miller 1999; Haiman & Menou 2000; Martini & Weinberg 2001; Hatziminaoglou et al. 2001; Wyithe & Loeb 2002, 2003; Hatziminaoglou et al. 2003) and semi-analytic (see, e.g., Cattaneo et al. 1999; Kauffmann & Haehnelt 2000; Cavaliere & Vittorini 2000; Cattaneo 2001; Cavaliere & Vittorini 2002; Enoki et al. 2003; Volonteri et al. 2003; Springel et al. 2005; Cattaneo et al. 2005) hierarchical models have been proposed to understand the QSO phenomenon. Most of these models successfully reproduce the QSO luminosity function [LF] at high (i.e. $z > 2$) redshifts, when the QSO activity reaches its peak, and some of them also account for the existence of QSO at very high (i.e. $z \sim 6$) redshift, hosting BHs as massive as $10^9 M_{\odot}$ (Volonteri & Rees 2005). However, hierarchical models generally fail to match the QSO properties at lower redshifts since the halo merger rate, which is generally regarded as the mechanism that triggers the QSO activity, declines with time less rapidly than the observed QSO number density. Various possible solutions have been proposed to solve this problem. For example it has been suggested that encounters within galaxy groups and clusters play a fundamental role in triggering the BH

accretion (Cavaliere & Vittorini 2000), that either the fraction of accreted gas or the time-scale of accretion depend on redshift (Haiman & Menou 2000; Cattaneo 2001), or that the accretion rate is proportional to the gas density of the host galaxy (Cattaneo et al. 2005). These solutions improve, with a different degree of success, the match to the observed LF at low redshift. The model proposed by Enoki et al. 2003 also allows to reproduce the QSO clustering, but is not guaranteed to match the correlation of Ferrarese (2002) between BH and halo mass. Another possibility, suggested by the outcome of high resolution, hydrodynamical simulations (Hopkins et al. 2005), is that of assuming that for a large fraction of its lifetime the QSO is heavily obscured by surrounding gas and dust except for a short window time of $\sim 10^7$ yr during which it shines at its peak luminosity.

In this work, we investigate to which extent ‘standard’ analytic and semi-analytic hierarchical models, where the assembly of supermassive black holes is related to the merger history of DM haloes, can reproduce both the observed QSO LF and their clustering at low redshifts. For this purpose we implement the two original analytic models of Wyithe & Loeb (2002) (WL02 hereafter) and Wyithe & Loeb (2003) (WL03 hereafter) and the semi-analytic one of Volonteri, Haardt & Madau (2003) (VHM hereafter), compare their predictions to the LF and clustering of the optical QSOs measured in various redshift catalogues, and discuss possible modifications to the models that improve the match to the data.

The outline of the paper is as follows. In Section 2 we present the observational datasets and the QSO properties relevant for our analysis. In Section 3 we present the WL02 and WL03 models, compare their predictions with observations and introduce some modification to the original models to better match the observed LF. A similar analysis is repeated in Section 4 for the semi-analytic model of VHM. Finally, in the last section we discuss our results and draw our main conclusions.

Throughout this paper we assume a flat Λ CDM cosmological model with Hubble constant $h = H_0/100 \text{ km s}^{-1} \text{ Mpc}^{-1} = 0.7$ and a dominant contribution to the density parameter from the cosmological constant, $\Omega_\Lambda = 0.7$. We adopt a CDM density power spectrum with primordial spectral index $n = 1$ and normalized by assuming $\sigma_8 = 0.9$.

2 DATASETS

The main dataset considered in this work is the QSO redshift catalogue by Croom et al. (2004) [C04 hereafter] obtained by merging the 2dF QSO Redshift Survey (2QZ), containing objects with an apparent b_j magnitude $18.25 < b_j < 20.85$, with the 6dF QSO Redshift Survey (6QZ) of bright ($16 < b_j < 18.25$) quasars. The full sample includes 23660 quasars in a wide redshift range ($0.3 < z < 2.9$) and spread over 721.6 deg^2 on the sky. The 2QZ/6QZ catalogue is affected by various types of incompleteness described in details by C04 that need to be accounted for in order to minimize systematic effects. For this purpose we have considered various subcatalogues, described below, characterized by a higher degree of completeness to allow a precise measurement of the QSO luminosity function [LF] and clustering properties.

A second dataset consisting of 5645 quasars with an apparent magnitude $18.0 < g < 21.85$ extracted from the recent 2dF-SDSS LRG and QSO [2SLAQ] survey (Richards et al. 2005, R05 hereafter) has also been considered to provide us with a reliable estimate of the LF of fainter objects at $z < 2.1$.

2.1 The QSO Optical Luminosity Functions

The 2QZ/6QZ catalogue has been used by C04 to compute the optical LF of a subsample of 15830 QSOs brighter than $M_{b_j} = 22.5$ in the redshift range $0.4 < z < 2.1$. The cut in absolute magnitude guarantees a minimum spectroscopic sector completeness of at least 70 per cent, while redshift constraints ensure a photometric completeness of 85 per cent. The LF has been evaluated into $\delta M_{b_j} = 0.5$ bins in absolute magnitude using the $1/V$ estimator of Page & Carrera (2000) into six equally spaced, independent redshift bins. The filled dots in the six panels of Fig. 1 show the LF of C04 measured in the different redshift intervals indicated in each plot.

In the same figure the thin solid line represents the best fit to the 2SLAQ LF determined by R05 in the same redshift intervals and b_j magnitude bins. The original g magnitudes have been transformed into b_j magnitudes by using the relation $\langle g - b_j \rangle = -0.045$ of R05. Finally, b_j magnitudes have been converted into B -band magnitudes by using the relation $M_B = M_{b_j} + 0.07$ of Porciani et al. (2004) [PMN hereafter].

2.2 QSO vs. Dark Matter Clustering

PMN have estimated the QSO two-point spatial correlation function of ~ 14000 2QZ/6QZ quasars with redshift $0.8 < z < 2.1$ in three different redshift intervals $[0.8, 1.3]$, $[1.3, 1.7]$ and $[1.7, 2.1]$. The three subsamples with median redshifts $z_{\text{eff}} = 1.06, 1.51, 1.89$ contain $\sim 4300, \sim 4700$ and ~ 4900 objects each. The more conservative cut in redshift and the use of these three redshift intervals guarantee (i) a photometric completeness larger than 90 per cent, (ii) a similar number of quasars in each redshift bin and (iii) that each subsample covers a similar interval of cosmic time.

PMN have measured the spatial two-point correlation function, $\xi^{\text{obs}}(r_\perp, \pi)$, using all QSO pairs separated by π along the line of sight and by r_\perp along the direction perpendicular to it and have computed the ‘projected correlation function’ Ξ by integrating ξ^{obs} along the π direction:

$$\frac{\Xi^{\text{obs}}(r_\perp)}{r_\perp} = \frac{2}{r_\perp} \int_0^{r_\perp} \xi^{\text{obs}}(r_\perp, \pi) d\pi. \quad (1)$$

Then, in order to quantify the QSO clustering with respect to the mass, they have evaluated the quasar-to-mass biasing function

$$b(r_\perp, z_{\text{eff}}) = \left[\frac{\Xi^{\text{obs}}(r_\perp, z_{\text{min}} < z < z_{\text{max}})}{\Xi_{\text{DM}}(r_\perp, z_{\text{eff}})} \right], \quad (2)$$

where z_{min} and z_{max} represent the lower and upper limits of the redshift interval and the projected mass correlation function, $\Xi_{\text{DM}}(r_\perp)$, was estimated as in Peacock & Dodds (1996). PMN have found that the QSO biasing function in Eq.(2) is almost independent of the projected separation r_\perp and thus it is possible to characterize the QSO spatial correlation properties at z_{eff} using a single ‘bias’ parameter $b(z_{\text{eff}})$. The results of the PMN analysis are presented in Fig. 2, where the filled dots show the value of $b(z_{\text{eff}})$ for the 2dF/6dF QSOs at three different redshifts, together with their 1σ uncertainty. The QSO-to-mass bias parameter $b(z_{\text{eff}})$ increases with redshift, in quantitative agreement with the results of a similar analysis performed by Croom et al. (2005).

3 ANALYTIC MODELS FOR THE QSO EVOLUTION

In this section we review the two analytic models by WL02 and WL03, use them to predict the QSO LF and clustering at $z < 2$ and

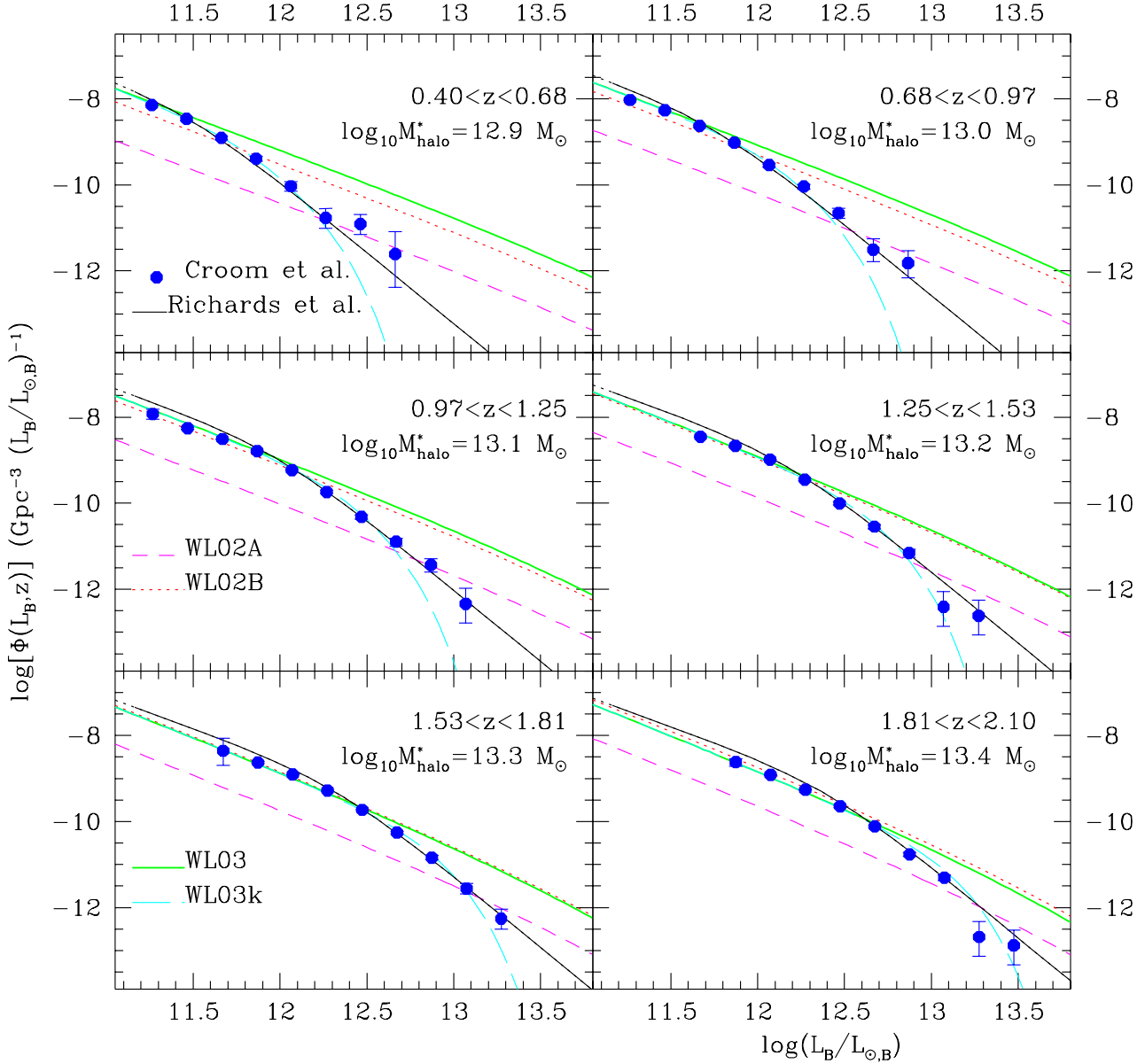


Figure 1. The QSO luminosity function in B -band at six different redshifts: models vs. observations. The filled circles show the 2dF/6dF QSO luminosity function measured by C04 together with their 1σ error bars. The thin solid line shows the best-fit to the 2SLAQ QSO luminosity function of R05. The short-dashed and the dotted lines show the WL02 model predictions obtained by setting $(\gamma = 4.71, \epsilon_0 = 10^{-5.1}, t_{dc,0} = 10^{6.3}\text{yr})$ (label: WL02A) and $(\gamma = 4.71, \epsilon_0 = 10^{-5.1}, t_{dc,0} = 10^{7.2}\text{yr})$ (label: WL02B), respectively. The thick solid line shows the WL03 model predictions obtained for $(\gamma = 5.0, \epsilon_0 = 10^{-5.7})$, while the thin long-dashed line (label: WL03k) represents the same model with an exponential cut in the luminosity-mass relation as in eq.(14), with $k = 0.77$ and M_{halo}^* indicated in the plots.

compare the results to the observations described in Sections 2.1 and 2.2. Since we apply these models beyond the redshift range they were originally designed for, we discuss and introduce some modifications to improve the fit to the 2dF/6dF and 2SLAQ LFs and clustering.

3.1 The WL02 model

The WL02 model describes the QSO evolution within the theoretical framework of hierarchical structure formation. However, in-

stead of associating the QSO activity to the formation of DM virialized haloes, as originally proposed by Haiman & Loeb (1998), it assumes that the QSO phenomenon is triggered by halo-halo mergers. The model also assumes that the mass of the BH powering the QSO, M_{bh} , is a fraction, ϵ , of the host halo mass M_{halo} and that, after a merging event, the QSO shines at the Eddington luminosity, L_{Edd} , with an universal light curve, $f(t)$. The B -band QSO luminosity can be related to M_{bh} and M_{halo} through $f(t)$:

$$L_B(t) = M_{\text{bh}}f(t) = \epsilon M_{\text{halo}}f(t) \quad \text{for } M_{\text{halo}} > M_{\text{min}}, \quad (3)$$

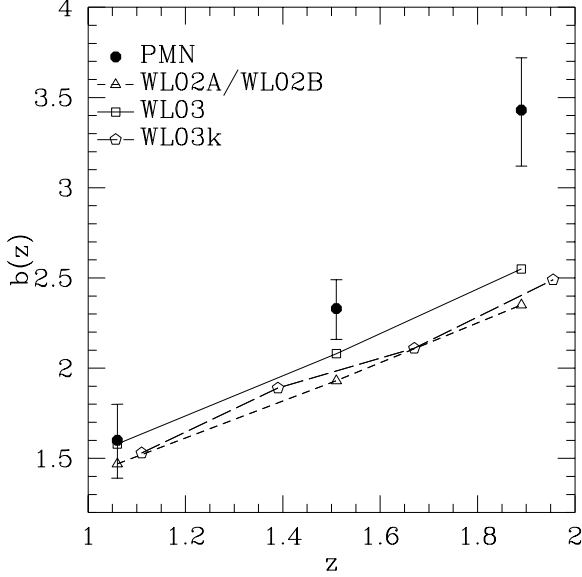


Figure 2. The mean QSO-to-mass biasing parameter, $b(z_{\text{eff}})$ estimated at three effective redshifts $z = 1.06$, $z = 1.51$ and $z = 1.89$: models vs. observations. The filled circles show the mean biasing of 2dF/6dF quasars measured by PMN with the associated 1σ uncertainties. The short-dashed line shows the theoretical predictions of the WL02 model with ($\gamma = 4.71$, $\epsilon_0 = 10^{-5.1}$, $t_{dc,0} = 10^{6.3}\text{yr}$) (label: WL02A) and with ($\gamma = 4.71$, $\epsilon_0 = 10^{-5.1}$, $t_{dc,0} = 10^{7.2}\text{yr}$) (label: WL02B). The amount and evolution of QSO biasing of these two models are exactly the same. The thick solid line shows the WL03 model predictions obtained for ($\gamma = 5.0$, $\epsilon_0 = 10^{-5.7}$) and the thin long-dashed line (label: WL03k) represents the same model with an exponential cut in the luminosity-mass relation as in eq.(14), with $k = 0.77$ and M_{halo}^* indicated in the plot.

where $M_{\text{min}} \sim 10^8 [(1+z)/10]^{-3/2} M_{\odot}$ is the minimum halo mass inside which a BH can form. The number density of active QSOs then can be obtained by multiplying the number of haloes with mass between ΔM_{halo} and $\Delta M_{\text{halo}} + d\Delta M_{\text{halo}}$ that accrete onto a halo of mass $M_{\text{halo}} - \Delta M_{\text{halo}}$ per unit time by the number density of haloes in the same mass range:

$$I(M_{\text{halo}}, \Delta M_{\text{halo}}) \equiv \left. \frac{dN(M, z)}{dM} \right|_{M=M_{\text{halo}} - \Delta M_{\text{halo}}} \times \left. \frac{d^2 N_{\text{merge}}}{d\Delta M_{\text{halo}} dt} \right|_{M=M_{\text{halo}} - \Delta M_{\text{halo}}} \quad (4)$$

The quantity $\frac{d^2 N_{\text{merge}}}{d\Delta M_{\text{halo}} dt}$ represents the merging rate predicted by the Extended Press-Schechter theory [EPS] Lacey & Cole (1993) and the halo mass function $\frac{dN(M, z)}{dM}$ is that of Sheth & Tormen (1999).

A further relation between M_{bh} and M_{halo} can be imposed by assuming that the scaling relation between the BH mass and the circular velocity of the host DM halo, v_c , observed by Ferrarese (2002) in the local universe, holds at all redshifts:

$$M_{\text{bh}} \propto v_c^\gamma = (159.4)^\gamma \left(\frac{M_{\text{halo}}}{10^{12} h^{-1} M_{\odot}} \right)^{\gamma/3} \times \left(\frac{\Omega_m(0)}{\Omega_m(z)} \frac{\Delta_c}{18\pi^2} \right)^{\gamma/6} (1+z)^{\gamma/2}, \quad (5)$$

where the second equality follows from the relation between v_c and M_{halo} (Barkana & Loeb 2001) in which $\Delta_c(z) = 18\pi^2 + 82d - 39d^2$, $d \equiv \Omega_m(z) - 1$ and $\Omega_m(z)$ represents the matter density pa-

rameter at a given redshift z . From eqs.(3) and (5):

$$\epsilon = \epsilon_0 \left(\frac{M_{\text{halo}}}{10^{12} M_{\odot}} \right)^{\gamma/3-1} \left(\frac{\Omega_m(0)}{\Omega_m(z)} \frac{\Delta_c}{18\pi^2} \right)^{\gamma/6} h^{\gamma/3} (1+z)^{\gamma/2}. \quad (6)$$

Finally, we assume that the QSO luminosity curve is given by a simple step function

$$f(t) = \frac{L_{\text{Edd},B}}{M_{\text{bh}}} \theta \left(\frac{\Delta M_{\text{halo}}}{M_{\text{halo}}} t_{dc,0} - t \right), \quad (7)$$

where $t_{dc,0} \ll H^{-1}(z)$ is the time of QSO duty cycle at $z = 0$.

Eqs.(5), (6) and (7) allow us to compute the QSO LF:

$$\Phi(L_B, z) = \int_{\epsilon M_{\text{min}}}^{\infty} dM_{\text{bh}} \int_0^{0.5\epsilon M_{\text{halo}}} d\Delta M_{\text{bh}} \times \int_z^{\infty} dz' \left. \frac{dN_{\text{bh}}}{dM} \right|_{M=M_{\text{bh}} - \Delta M_{\text{bh}}} \left. \frac{d^2 N_{\text{merge}}}{d\Delta M_{\text{bh}} dt} \right|_{M=M_{\text{bh}} - \Delta M_{\text{bh}}} \times \frac{dt'}{dz'} \delta[L_B - M_{\text{bh}} f(t_z - t')] \quad (8)$$

that, once integrated over M_{bh} , has an analytic expression that depends on the three free parameters $t_{dc,0}$, ϵ_0 and γ :

$$\Phi(L_B, z) = \int_0^{0.5M_{\text{halo}}} d\Delta M_{\text{halo}} \frac{3}{\gamma \epsilon} \frac{t_{dc,0}}{5.7 \times 10^3} \frac{\Delta M_{\text{halo}}}{M_{\text{halo}}} \times I(M_{\text{halo}}, \Delta M_{\text{halo}}), \quad (9)$$

where $M_{\text{halo}} = L_{\text{Edd},B} / (5.7 \times 10^3 \epsilon L_{\odot,B}) M_{\odot}$.

The connection between QSO luminosity and halo mass in our model, $L_B(M_{\text{halo}})$, and the existence of analytic models that describe the spatial and clustering of DM haloes (see, e.g., Mo & White 1996; Sheth & Tormen 1999) allow us to investigate the spatial correlation properties for QSOs. In particular, we can compute the QSO-to-mass biasing parameter, $b(z)$, averaged over all QSO luminosities:

$$b(z) = \frac{\int_{L_{B,\text{min}}}^{\infty} b(L_B(M_{\text{halo}}), z) \Phi(L_B, z) dL_B}{\int_{L_{\text{min},B}}^{\infty} \Phi(L_B, z) dL_B}, \quad (10)$$

where $\Phi(L_B, z)$ is the QSO LF in Eq.(9), $L_{B,\text{min}}$ is the luminosity of the faintest object in the sample. The quantity $b(L_B(M_{\text{halo}}), z)$ represents the biasing parameter of a halo of mass M_{halo} hosting a QSO of luminosity L_B at the redshift z that has been computed by Sheth & Tormen (1999):

$$b(L_B(M_{\text{halo}}), z) = 1 + \frac{1}{\delta_c(0)} \left[\frac{a\delta_c^2(z)}{\sigma_M^2} - 1 \right] + \frac{2p}{\delta_c(0)} \left(\frac{1}{1 + [\sqrt{a}\delta_c(z)/\sigma_M]^{2p}} \right), \quad (11)$$

where $a = 0.707$, $p = 0.3$, $\delta_c(z)$ is the critical threshold on the linear overdensity for spherical collapse at redshift z and σ_M^2 is the rms linear density variance smoothed with a ‘top-hat’ filter corresponding to the mass M . Eq.(10) provides us with an analytic expression for $b(z)$. It assumes a univocal relation between quasar luminosity and halo mass, or, in other words, that the probability of finding a quasar of a given luminosity L_B in a halo of mass M_{halo} depends on M_{halo} only.

3.2 WL02 model vs. observations

Let us now compare both the QSO LF and the biasing parameter predicted by the WL02 model to the various datasets available. Given the background cosmology, the model predictions are

fully specified by a set of three parameters: $(\gamma, \epsilon_0, t_{dc,0})$. Here we explore two separate cases. The first one, which is slightly different from the one considered in the original WL02 paper (and labeled WL02A in Figs. 1 and 2), uses the parameters $(\gamma = 4.71, \epsilon_0 = 10^{-5.1}, t_{dc,0} = 10^{6.3} \text{ yr})$. The first two chosen values represent the best fit to the observations of Ferrarese (2002), while the latter, which corresponds to a value of $t_{dc}(z=3) = 10^{6.9} \text{ yr}$ at $z \sim 3$, is fully consistent with the lifetime of bright QSOs, $t_{dc}(z \simeq 3) = 10^7 \text{ yr}$, inferred from the sample of Lyman-break galaxies of Steidel et al. (2002). The predicted QSO LFs, plotted as short-dashed line in Fig. 1, fail to match the observed LF both in the bright and the faint ends. This result is similar to the one originally obtained by WL02 using the set of parameters $(\gamma = 5.0, \epsilon_0 = 10^{-5.4}, t_{dc,0} = 10^{6.3} \text{ yr})$, that constitutes their best fit to the data. Since the overall amplitude of the model LF (Eq. 9) linearly depends on $\gamma^{-1}, \epsilon_0^{-1}$ and $t_{dc,0}$, it is quite straightforward to boost up the model LF to match the number density of the observed QSOs. For example, fixing the values of $\gamma = 4.71, \epsilon_0 = 10^{-5.1}$, and leaving $t_{dc,0}$ as a free parameter, we find a best fit for $t_{dc,0} = 10^{7.2} \text{ yr}$. The resulting model, labeled WL02B, is shown in Fig. 1 as a dotted line. This duty-cycle is very large and some *ad hoc* modifications to the WL02 model would be required to satisfy the high-redshift constraints of Steidel et al. (2002). We will discuss physically motivated modifications to the WL02 model later on in the framework of the WL03 model.

The biasing functions predicted by the WL02A and WL02B models are shown in Fig. 2 at three different redshifts and compared to the PMN data. The line-styles are the same as in Fig. 1. The two models predict the same amount and evolution of QSO biasing. In both cases at $z = 1.06$, QSOs are mildly biased with respect to the underlying mass, marginally consistent with observations, while their clustering at $z = 1.89$ is significantly less than observed.

3.3 The WL03 model

WL03 modified the original WL02 model by prescribing a self-regulated accretion mechanism of SBHs following *major* mergers between haloes of different masses, as proposed by Kauffmann & Haehnelt (2000). A self-regulated accretion mechanism is the natural outcome of the production of powerful gas winds that interrupt the infall of gas on the BH after halo mergers. Self-regulation takes place when the energy in the outflow equals the gravitational binding energy in a dynamical time (Silk & Rees 1998). Assuming that the gas is located in a disk with characteristic radius $\sim 0.035 r_{\text{vir}}$, the dynamical time t_{dyn} is given by

$$t_{\text{dyn}} = 0.035 \frac{r_{\text{vir}}}{v_c} = \frac{3.64 \times 10^7}{h} \left(\frac{\Omega_m(0)}{\Omega_m(z)} \frac{\Delta_c}{18\pi^2} \right)^{-1/2} \times (1+z)^{-3/2} \text{yr}, \quad (12)$$

and represents the quasar duty cycle: $t_{dc} = t_{\text{dyn}}$. The major merger condition has been introduced to guarantee that the dynamical friction time-scale (Binney & Tremaine 1987) for the satellite is shorter than a Hubble time. For this reason WL03 only considered mergers between haloes with a mass ratio $P \equiv \Delta M_{\text{halo}}/M_{\text{halo}} > 0.25$. As a consequence, the model LF can be expressed as

$$\Phi(L_B, z) = \int_{0.25M_{\text{halo}}}^{0.5M_{\text{halo}}} d\Delta M_{\text{halo}} \frac{3}{\gamma \epsilon} \frac{t_{\text{dyn}}}{5.7 \times 10^3} \times I(M_{\text{halo}}, \Delta M_{\text{halo}}). \quad (13)$$

It only depends on two free parameters: ϵ_0 and γ . The model biasing function has been computed using Eq.(10).

3.4 WL03 model vs. observations

The first model we have explored is the one by WL03 corresponding to the choice of parameters $(\gamma = 5.0, \epsilon_0 = 10^{-5.7})$, still consistent with the observational data of Ferrarese (2002). The model LF (labeled WL03 and plotted with a thick solid line in Fig. 1) is very similar to that of WL02B, but has the advantage of having a physically, well motivated QSO duty-cycle. The WL03 LF matches the observed one at low luminosities, but it overpredicts the number density of bright QSOs. This discrepancy is more evident at low redshifts and can be accounted for by modifying the WL03 model. One possibility is to allow for a major merger threshold P that depends on M_{halo} . As we have checked, it is indeed possible to find some suitable function $P(M_{\text{halo}})$ monotonically increasing with M_{halo} that allows to match both the faint and bright ends of the observed QSO LF. While this is somewhat an *ad hoc* solution, a more physically plausible modification has been proposed by WL03 and consists of assuming that accretion onto BH is hampered by the high temperature of the gas within group/cluster-size haloes. WL03 proposed that accretion onto the central BH should be prevented within haloes of masses larger than $10^{13.5} M_{\odot}$, corresponding to a $L \sim 2 \times 10^{13} L_{\odot,B}$ at $z \simeq 1$. We have made a similar assumption and proposed that the accretion efficiency decreases above a given critical halo mass resulting in a modified relation between L_{QSO} and M_{halo} :

$$L_{\text{QSO}} = \tilde{L} (1 - \exp(-(L^*/\tilde{L})^k)). \quad (14)$$

In the previous equation $\tilde{L} = 5.7 \times 10^3 \epsilon (M_{\text{halo}}/M_{\odot})$ is the *B*-band Eddington luminosity of the original WL03 model and L^* is the Eddington luminosity of a halo with critical mass M_{halo}^* . Both k and M_{halo}^* can be treated as free parameters. The thin dashed line in Fig. 1 shows the effect of a keeping $k = 0.77$ while leaving M_{halo}^* as a free parameter, whose value is indicated in the plots. The LF predicted by the model (labeled WL03k) provides a good match to the observed one at all redshifts, except perhaps for very bright objects. The resulting values of M_{halo}^* range between $10^{12.9}$ and $10^{13.4} M_{\odot}$ which constitute plausible values, close to that proposed by WL03. Leaving also k as a free parameter does not improve significantly the agreement with the observational data and a best fit value close to $k = 0.77$ is found at all redshifts. We have also tried to use the model WL03 without the restriction to major mergers, but it has resulted inconsistent with the data by about several orders of magnitude and we have decided not to show it.

4 SEMI-ANALYTIC MODELS FOR THE HIERARCHICAL EVOLUTION OF QUASARS

Semi-analytic approaches to the evolution of QSOs in a hierarchical scenario also assume some relation between QSOs and DM haloes properties. However, they differ from analytic modeling since the evolution of DM haloes and of the QSOs within them are treated separately. The merging history of DM haloes is described by the EPS formalism. Phenomenological relations are used to model the physical processes leading to the quasar evolution. It is therefore possible to adopt a more detailed description of the physics involving the baryonic component of cosmic structures, including BHs. A second advantage of the semi-analytic approach is the flexibility of the scheme, so that different astrophysical prescriptions can

be tested within the same framework of cosmic evolution of DM haloes.

4.1 The VHM model

In this work we focus on the semi-analytic model developed by VHM that describes the hierarchical assembly, evolution and dynamics of the BHs powering QSOs (Volonteri, Haardt & Madau 2003; Volonteri, Madau & Haardt 2003; Madau et al. 2004; Volonteri & Rees 2005). Like WL02 and WL03, VHM also assume that: (i) the observed correlation between BH masses and circular velocity (Ferrarese 2002) justifies the assumption of a link between QSO activity and haloes' properties and constitutes a constraint to the semi-analytic model at $z = 0$, and that (ii) the cosmological evolution of DM haloes is well described by the EPS theory. Moreover, like in the WL03 case, they further assume that (iii) the QSO activity is triggered by major mergers.

The numerical implementation of the semi-analytic model consists of a two-step procedure. The first step is aimed at constructing a set of halo merging histories using the EPS theory. In the EPS formalism, when one takes a small step δz back in time, the number of progenitors a parent halo of mass M_0 at $z = z_0$ fragments into is (Lacey & Cole 1993):

$$\frac{dN}{dM}(z = z_0) = \frac{1}{\sqrt{2\pi}} \frac{M_0}{M} \frac{1}{S^{3/2}} \frac{d\delta_c}{dz} \frac{d\sigma_M^2}{dM} \delta z, \quad (15)$$

where $S \equiv \sigma_M^2(z) - \sigma_{M_0}^2(z_0)$, $\sigma_M^2(z)$ and $\sigma_{M_0}^2(z_0)$ are the linear theory rms density fluctuations smoothed with a 'top-hat' filter of mass M and M_0 at redshifts z and z_0 , respectively, and $\delta_c(z)$ is the critical thresholds on the linear overdensity for spherical collapse at redshift z . Integrating this function over the range $0 < M < M_0$ gives unity: all the mass of M_0 was in smaller subclumps at an earlier epoch $z > z_0$. From Eq.(15) we can compute a fragmentation probability that, via rejection methods, can be used to construct a binary merger tree. Implementing a successful Monte Carlo procedure, however, requires the use of two different numerical approximations (Somerville & Kolatt 1999). First of all, since in a CDM cosmology the number of haloes diverges as the mass goes to zero, it is necessary to introduce a cut-off mass, M_{res} , that marks the transition from resolved progenitors (having $M > M_{\text{res}}$) to the accreted mass that accounts for the cumulative contribution of all mass accreted from unresolved haloes. Secondly, the time-step δz has to be small enough to guarantee a small mean number of fragments N_p in the range $M_{\text{res}} < M < M_0/2$, to avoid multiple fragmentation.

Once the appropriate choices for δz and M_{res} are made, the binary tree is constructed by using a Monte Carlo procedure similar to that of Cole et al. (2000), described in VHM. We have taken $M_{\text{res}} = 10^{-3}M_0$ at $z = 0$ decreasing with redshift as $(1+z)^{3.5}$. Finally, for each Monte Carlo realization we have used 820 time-steps logarithmically spaced between $z = 0$ and $z = 20$. As shown by VHM, with this parameter choice our merger tree algorithm not only conserves the mass, but also reproduces the EPS conditional mass function at all redshifts.

In the second step of the procedure, we implement a set of analytic prescriptions and follow the accretion history of massive BHs within their host haloes to model the QSO activity. The VHM model assumes that the seed BHs formed with masses of $150M_\odot$ (note that, as shown by VHM, the final results are not very sensitive to this choice) following the collapse of the very rare Pop III stars, in minihaloes forming at $z = 20$ from the density peaks above a 3.5σ threshold. In the assumed Λ CDM cosmology this corresponds to minihaloes with mass $\sim 1.6 \times 10^7 M_\odot$. Then we assume that the

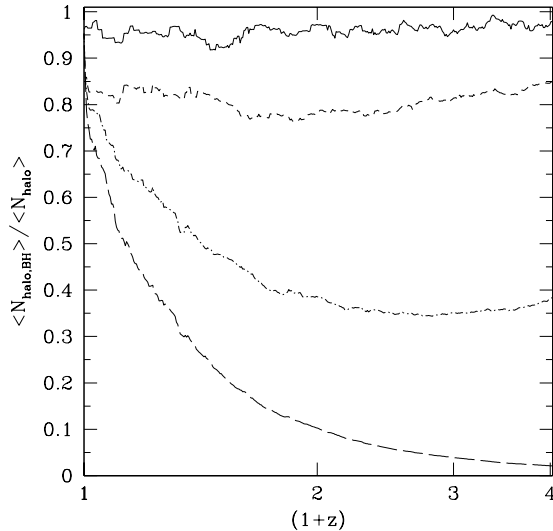


Figure 3. Fraction of haloes hosting at least a nuclear massive BH vs. redshift. The long-dashed curve shows the occupation fraction computed by weighting over all branches of the merger trees. The occupation fraction increases with increasing halo mass: $M_{\text{halo}} > 10^{10}M_\odot$ (dot-dashed curve), $M_{\text{halo}} > 10^{11}M_\odot$ (short-dashed curve) and $M_{\text{halo}} > 10^{12}M_\odot$ (solid curve).

quasar activity is triggered only by major mergers with $P > 0.1$, a threshold lower than $P > 0.25$ adopted by WL03.

Two main features differentiate the VHM model from the WL03 one. First, the VHM model is naturally biased, as the BH seeds are associated with high-density peaks in the fluctuations field. Second, VHM take into account the dynamical evolution of BHs, including strong gravitational interactions such as the gravitational rocket effect (Merritt et al. 2004; Volonteri & Perna 2005). Such dynamical interactions can possibly eject BHs at high velocities from the centre of haloes. The net effect is to contribute to selecting massive haloes (i.e. those with a large escape velocity) as BH hosts. In all three scenarios we consider (see below), we have included a treatment of the 'gravitational rocket' effect following Favata et al. (2004) and Merritt et al. (2004) (upper limit to the recoil velocity). More details can be found in Volonteri & Perna (2005). Fig. 3 shows the occupation fraction, i. e. the fraction of haloes hosting nuclear BHs for haloes of different masses. The occupation fraction of large haloes ($M_{\text{halo}} > 10^{12}M_\odot$) is of order unity at all times, while smaller haloes have a large probability of being deprived of their central BH.

Following a major merger, the BH at the centre of the massive progenitor can grow in mass in two ways: (i) after a dynamical friction time when a bound BH binary system forms at the centre of the halo, hardens via three body interactions (Quinlan 1996; Milosavljević & Merritt 2001) and then rapidly coalesces through the emission of gravitational waves (Peters 1964); (ii) after a dynamical free-fall time when a significant fraction of the gas falls to the centre of the merged system (Springel et al. 2005; Di Matteo et al. 2005) and is accreted on the BH at an appropriate rate. Yet, as shown by VHM, the first mechanism contributes little to the BH mass accretion and will be neglected in this work. To implement the second mechanism we need to specify the prescription for the mass accretion and its rate. We have explored three different scenarios. The first two assume that BHs start accreting mass at the

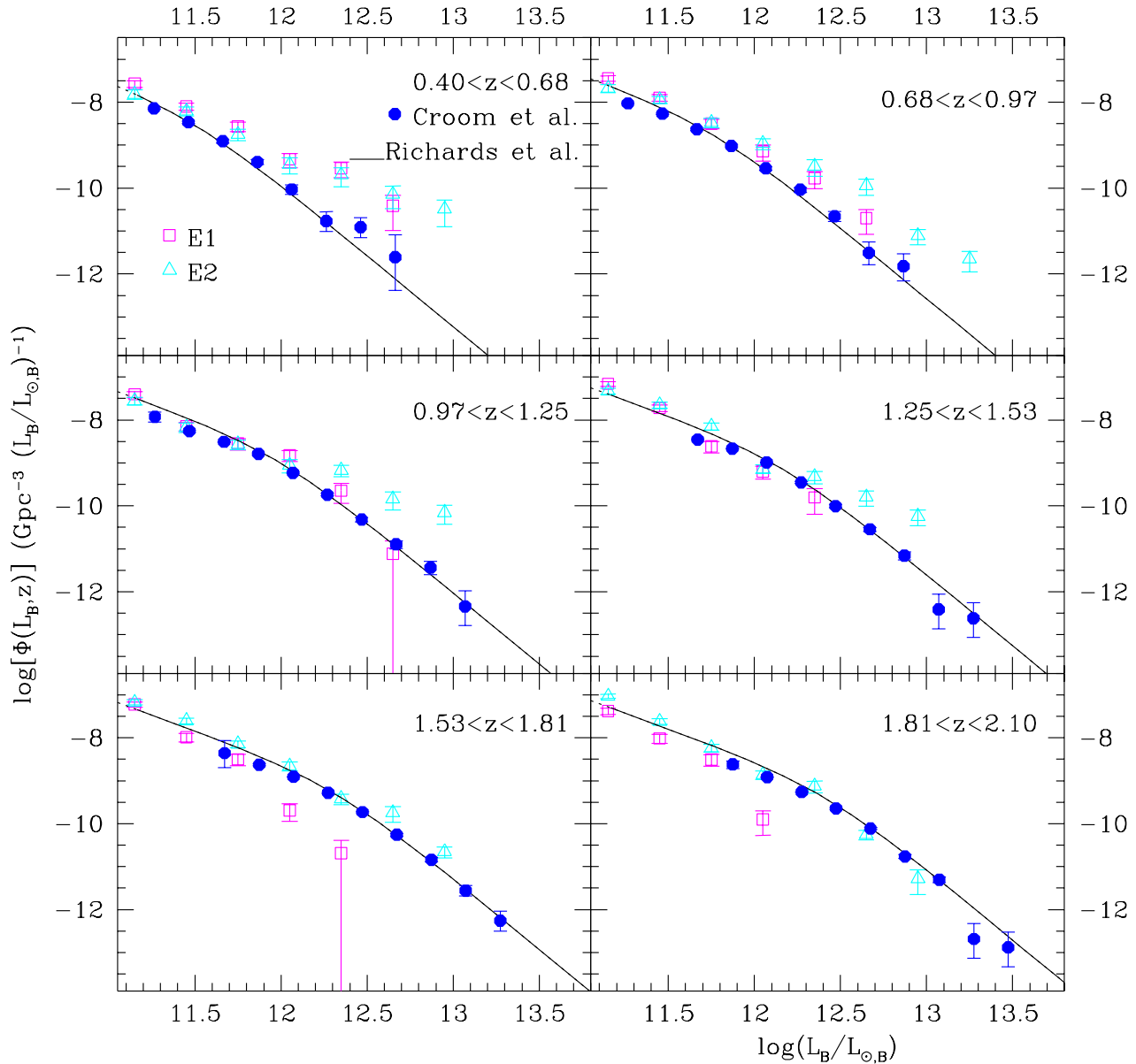


Figure 4. The QSO luminosity function in B -band at six different redshifts: models vs. observations. The filled dots show the 2dF/6dF QSO luminosity function measured by C04 together with their 1σ error bars. The thin solid line shows the best fit to the 2SLAQ QSO luminosity function of R05. The open squares refer to the VHM model predictions when a fraction $\alpha = 7 \times 10^{-6}$ of accreted mass of the merged system total mass is assumed. The open triangles show the VHM model predictions when a relation between the accreted mass and the circular velocity of the host halo is assumed.

Eddington rate after about one dynamical free-fall timescale from the merger. Accretion lasts until a mass ΔM_{accr} has been added to the BH, but, as in VHM, we have inhibited gas accretion in all haloes with $v_c > 600 \text{ km s}^{-1}$.

In the first of the two scenarios, labeled E1, the accreted mass is proportional to the mass of the available gas and hence to the total mass of the massive progenitor: $\Delta M_{\text{accr}} = \alpha M_{\text{halo}}$. Here, $\alpha = 7 \times 10^{-6}$ guarantees the normalization of the $M_{\text{bh}} - \sigma_g$ relation at $z = 0$, where σ_g is the velocity dispersion of the host galaxy (Tremaine et al. 2002), scaling with the circular velocity of the halo as suggested by Ferrarese (2002). No feedback is ex-

plicitly included in the semi-analytic scheme. As $M_{\text{halo}} \propto v_c^3$, the slope of the $M_{\text{bh}} - \sigma_g$ relation is flatter than the observed one (but see Wyithe & Loeb 2005a). This scenario is similar in spirit to the WL03 model, and is meant to compare the clustering properties of quasars at low redshift to that of their higher redshift counterparts. Adelberger & Steidel (2005) indeed find that the clustering of active nuclei at $2 \lesssim z \lesssim 3$ points to a $M_{\text{bh}} - M_{\text{halo}}$ relation which is independent of redshift.

The second scheme [E2] assumes a scaling relation between the accreted mass and the circular velocity of the host halo, $\Delta M_{\text{accr}} = k \times v_c^5$, which is normalized *a-posteriori* to reproduce the

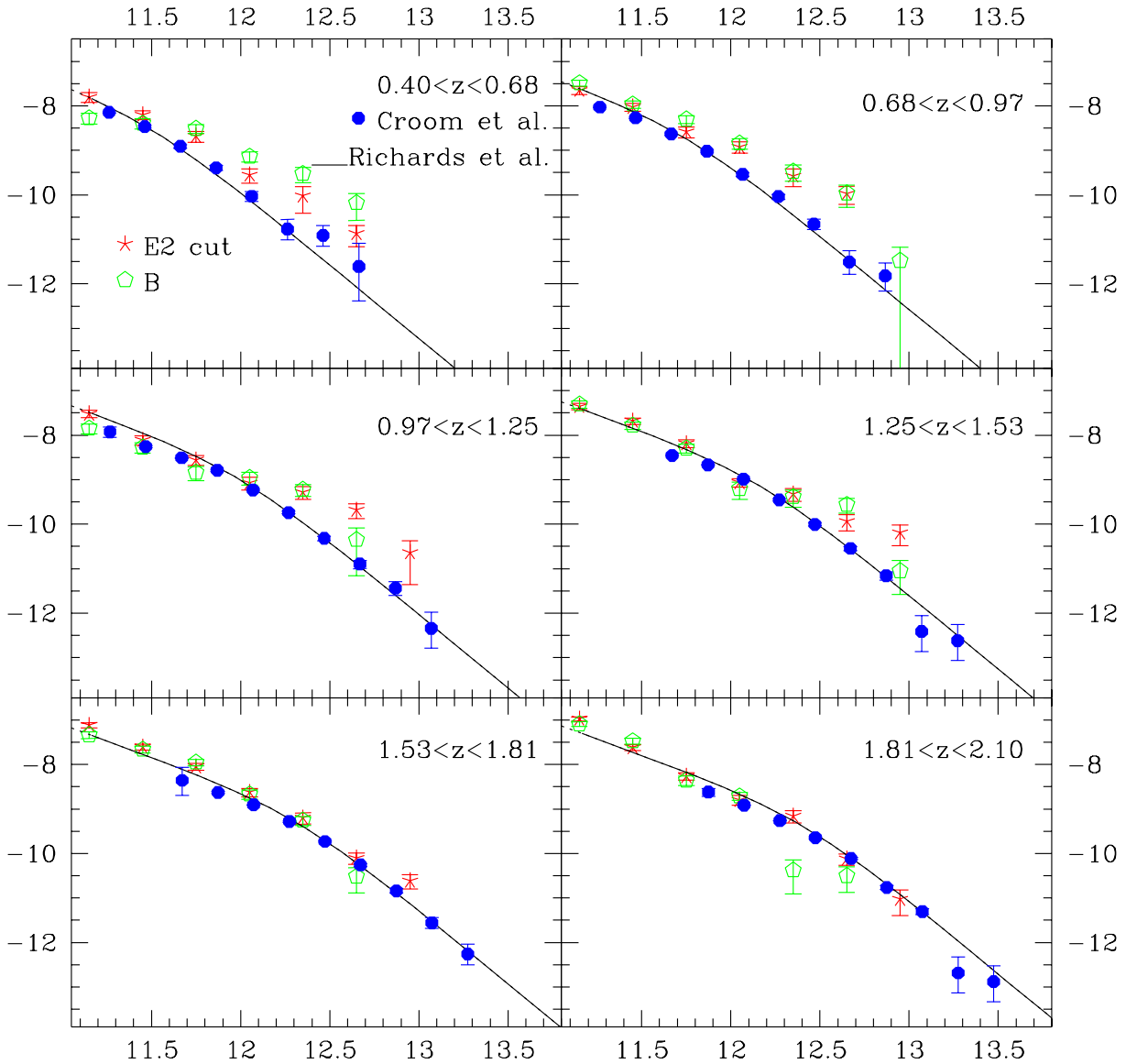


Figure 5. The QSO luminosity function in B -band at six different redshifts: models vs. observations. The filled dots show the 2dF/6dF QSO luminosity function measured by C04 together with their 1σ error bars. The thin solid line shows the best fit to the 2SLAQ QSO luminosity function of R05. The open pentagons refer to the VHM model predictions including super-critical accretion in high- z haloes. The asterisks show a model in which the accreted mass scales with the circular velocity of the host halo, and accretion is suppressed in haloes with $M_{\text{halo}} > 10^{13.5} M_{\odot}$.

observed relation between M_{bh} and v_c at $z = 0$ (Ferrarese 2002). VHM showed that this scenario overestimates the optical LF at $z < 1$. Here, we assume a linear dependence of k on redshift, as $k = k(z) = 0.15(1+z) + 0.05$, to account for the decrease of the gas available to fuel BHs. The above relation is totally empirical and was determined iteratively in order to get a better fit to the LF, without underestimating the local SBH mass density.

The last prescription for mass accretion, labeled B, assumes an early stage of super-critical accretion during which the central BH accretes mass at a rate that can be estimated by the Bondi-Hoyle formula (Bondi & Hoyle 1944). This model applies to metal-free

haloes, therefore we assume that by $z = 12$ the interstellar medium has been enriched, and we inhibit super-critical accretion rates. When the super-critical phase ends, accretion proceeds in subsequent episodes as in model E2. This possibility has been recently advocated by Volonteri & Rees (2005) to reconcile a hierarchical evolution with the existence of QSO at $z \sim 6$, hosting SBHs with masses $\sim 10^9 M_{\odot}$.

The end product of our semi-analytic models is a set of merging and accretion histories for 220 parent haloes with masses in the range ($1.43 \times 10^{11} M_{\odot}, 10^{15} M_{\odot}$). When active, i.e. during the period of mass accretion, the QSO shines with a B -band luminosity of

$(L_B/L_\odot) = M_{\text{bh}} \times 10^{3.46} M_\odot$, obtained under the assumptions that the rest mass is converted to radiation with a 10 per cent efficiency and that only a fraction $f_B = 0.08$ of the bolometric power is radiated in the blue band. Finally quasars in the model outputs are selected according to the 2dF/6dF criteria.

The model QSO LF at different redshifts has been computed by evaluating the number density of active QSOs in each luminosity bin in redshift intervals centred on an effective redshift z_{eff} . In practice we have counted the number of active QSOs in the redshift and luminosity bins in all merger trees, each of them weighted by the number density of their parent haloes at $z = 0$ [evaluated using the Sheth & Tormen (1999) formula]; the result has been normalized using the number of time-steps in the redshift interval and the number of merger trees considered. Associate uncertainties have been computed by assuming Poisson statistics.

The biasing function $b(z)$ at the three redshifts considered by PMN has been estimated by using the following equation

$$b(z) = \frac{\int_0^{+\infty} b(M_{\text{halo}}, z) \Psi(M_{\text{halo}}(L_B > L_{\text{min},B}), z) dM_{\text{halo}}}{\int_0^{+\infty} \Psi(M_{\text{halo}}(L_B > L_{\text{min},B}), z) dM_{\text{halo}}}, \quad (16)$$

where $\Psi(M, z)$ is the mass function of the haloes hosting QSOs with luminosities larger than the selection thresholds of PMN ($L_{B,\text{min}}/L_{\odot,B} = \{1.5 \times 10^{11}, 3.9 \times 10^{11}, 6.6 \times 10^{11}\}$), and $b(M_{\text{halo}}, z)$ is the bias function of haloes computed following Sheth & Tormen (1999).

Model predictions also allow a straightforward evaluation of the mean halo occupation number, i.e. the average number of active QSOs hosted in haloes with mass between M_{halo} and $M_{\text{halo}} + dM_{\text{halo}}$:

$$N_{\text{QSO}}(M_{\text{halo}}) = \frac{\Psi(M_{\text{halo}})}{dN/dM_{\text{halo}}}, \quad (17)$$

where $\Psi(M_{\text{halo}})$ is the mass function of haloes hosting active quasars in the halo merger trees and dN/dM_{halo} is the Sheth & Tormen (1999) halo mass function. Model uncertainties have been evaluated from Poisson errors associated to $\Psi(M_{\text{halo}})$.

4.1.1 VHM model vs. observations

In Figs. 4 and 5 we compare our model LF with the observations. The 6dF/2dF and the 2SLAQ QSO LFs are plotted using the same symbols as in Fig. 1. The LFs predicted by our semi-analytic models are plotted with the three different symbols indicated in the plot. At low redshifts all models reproduce the faint end of the LF fairly well. However, they systematically overpredict the number of bright QSOs: this indicates that having inhibited gas accretion in haloes with $v_c > 600 \text{ km s}^{-1}$ has little impact on our results. Indeed, this circular velocity is significantly larger than that associated to the mass threshold $M_{\text{halo}}^* \sim 10^{13.5} M_\odot$ adopted in the WL03K model. Imposing a similar mass threshold in the VHM model (model E2_{cut}), in place of the $v_c > 600 \text{ km s}^{-1}$ cut-off, we find a much better agreement between the model predictions and the observed LF at all $z < 1.5$. Finally, we note that model E1 fails to produce QSOs brighter than $10^{12} L_{\odot,B}$.

As shown in Fig. 6, all semi-analytic models explored match the observed biasing function out to $z \sim 2$. We notice that the three semi-analytic models explored predict a very similar biasing function. As pointed out by Wyithe & Loeb (2005a), the evolution of clustering is slightly faster when the BH mass scales with the halo

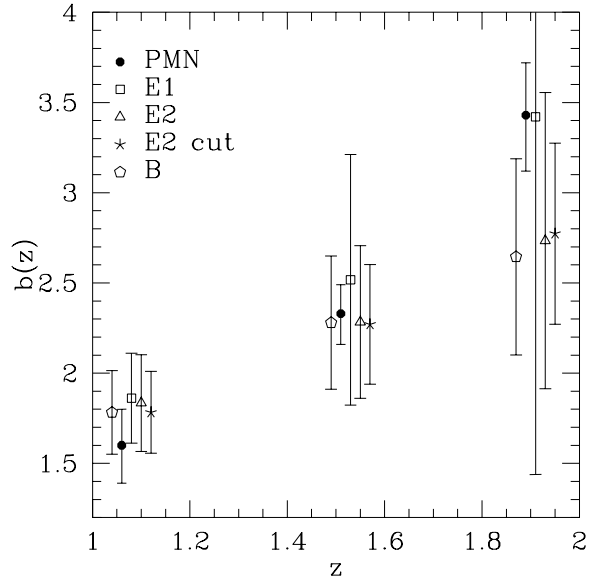


Figure 6. The mean QSO-to-mass biasing parameter, $b(z_{\text{eff}})$ estimated at three effective redshifts $z = 1.06$, $z = 1.51$ and $z = 1.89$: models vs. observations. The filled circles show the mean biasing of 2dF/6dF quasars measured by PMN. Symbols are as in Figs. 4 and 5.

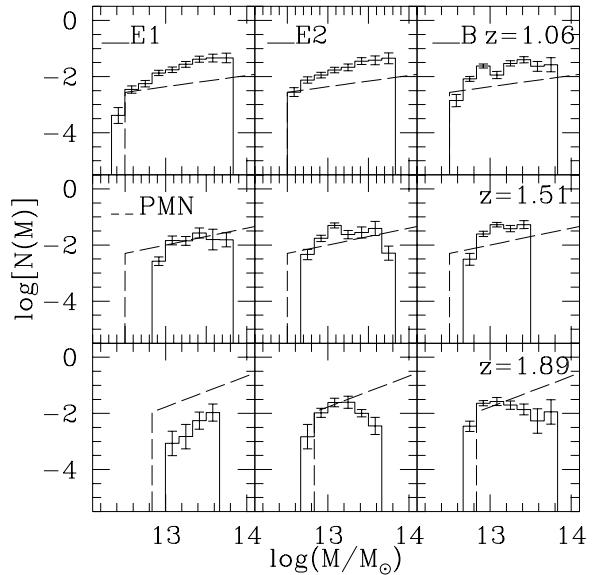


Figure 7. The mean halo occupation number of QSO at three effective redshifts $z = 1.06$, $z = 1.51$ and $z = 1.89$ (from top to bottom). Histograms represent model predictions, while the dashed line shows the mean halo occupation number proposed by PMN and consistent with 2dF/6dF QSO data. Left panels: model E1. Central panels: model E2. Right panels: model B.

mass (model E1) rather than the circular velocity (model E2), although the difference is of little significance given the large scatter in the model predictions.

The reason of the difference can be understood by looking at the histograms plotted in Fig. 7 representing the mean halo occupation number, $N_{\text{QSO}}(M_{\text{halo}})$, of the various models. At $z = 1.89$ model E1 exhibits a steeper dependence on halo mass compared

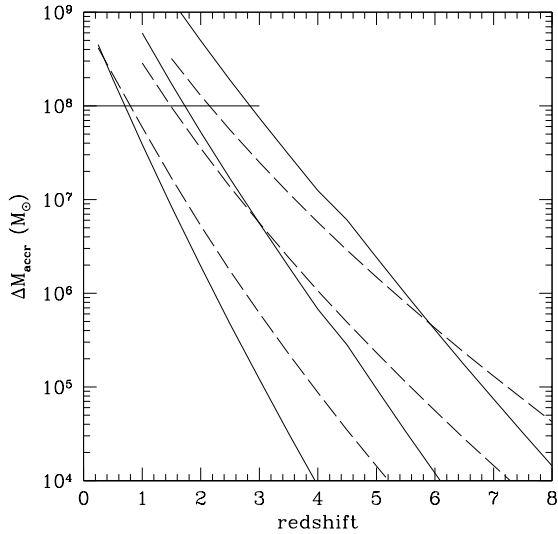


Figure 8. Accreted mass as a function of redshift for different halo masses. From top to bottom, curves are for 2.5σ , 2σ and 1.5σ peak haloes. Dashed curves: model E1. Solid curves: model E2. The horizontal line shows the BH mass corresponding to $L_{B,\min}$ at $z = 1.89$ of PMN, assuming Eddington accretion rate.

to the other cases meaning that QSOs are preferentially found in massive haloes with a high degree of spatial clustering. This result derives from the fact that the accretion scheme of model E1 is more efficient at very high redshift ($z > 6$) than that of model E2, due to the different scaling of ΔM_{accr} with redshift. Fig. 8 exemplifies this effect. On one hand, ΔM_{accr} is a steeper function of redshift in model E2, implying that massive BHs accrete more mass in every accretion episode, thus leading to a longer duty-cycle, and a larger occupation number, in general. On the other hand, at redshift $z = 1.89$, only quasars above $L_{B,\min}$ are selected. In model E2 the 2σ -peak haloes contain BHs massive enough to be above threshold, while for model E1 a slightly more massive halo is needed. Consequently this enhances the bias. At lower redshifts this effect becomes progressively less important. This result interestingly agrees with that of Adelberger & Steidel (2005): at $z > 2$ SMBH masses correlate with the halo mass instead of with velocity dispersion, or circular velocity. We can speculate that there might be a transition in the interaction between SMBHs and their hosts, which switches on at $z \simeq 2$: at higher redshifts the SMBH mass scales with the halo mass, at lower redshifts with its velocity. As shown in Fig. 8, the accreted mass in a given episode is larger in model E1 than in model E2 for haloes representing density peaks below 2σ at $z > 3$. Model E1, therefore, implies an earlier growth for SMBHs.

On the contrary, model B, in which massive BHs accrete mass with very high efficiency at high redshifts preferentially populate smaller haloes. Massive BHs in more massive haloes have already grown to masses close to the $M_{\text{bh}} - \sigma_g$ threshold. At $z = 1.06$ all models, especially E1, predicts a number of QSOs in haloes which is systematically larger than the one inferred from PMN, especially in high-mass haloes. This discrepancy, which is marginally significant, considering the errors estimated by PMN, reflects the fact that semi-analytic models overestimate the optical LF of bright quasars at low redshifts, as shown in the top panels of Figs. 4 and 5. On the other hand, at high redshifts all models predict a halo occupation

number that is systematically smaller than the PMN one, which again reflects the fact that our model LFs slightly underestimate the observed one at high redshifts (Figs. 4 and 5, bottom panels). This effect is particularly evident for model E1, which, as we have noticed before, predicts no QSOs with $L > 10^{12} L_{\odot,B}$ at $z > 1.25$.

5 DISCUSSION AND CONCLUSIONS

In this work, we have carried out for the first time a systematic study aimed at assessing how well, within the framework of hierarchical build up of supermassive black holes and massive halos hosts, analytic and semi-analytic techniques perform in reproducing the QSO luminosity function and spatial distribution at very low redshifts, bound to reproduce the relation between M_{bh} and M_{halo} (Ferrarese 2002). We have found that only minor, physically-motivated modifications to standard semi-analytic techniques are required to match observations at redshifts as small as 0.5. More profound modifications seem to be required for a successful modeling of the very local QSO population.

Previous studies, like those performed by WL02, WL03 and VHM, have shown that analytic and semi-analytic models well reproduce the observed QSO LF at high redshifts. At low redshifts, however, these methods systematically overpredict the number density of bright objects; a mismatch that becomes increasingly large when decreasing the redshift. To improve the fit to the data we have proposed two simple modifications to the original WL02, WL03 and VHM models. The first possibility is to assume that the major merger threshold required to trigger the QSO activity depends on the mass of the hosting halo. This reduces the number density of bright QSOs that can only be activated by rare merging events between large haloes of similar masses. A second possible modification is physically motivated by the fact that gas accretion is expected to be inefficient within large haloes due to the high temperature of the baryons: this can inhibit accretion in haloes larger than $\sim 10^{13.5} M_{\odot}$, hence reducing the abundance of bright objects. Both prescriptions significantly improve the fit to the bright end of the QSO LF, especially when implemented within the analytic framework. Yet, significant discrepancies still remain, especially at very low redshifts, that could be possibly eliminated by including two more factors that are missing from the models.

First, when comparing our model predictions to the observed B -band QSO LF, we have implicitly ignored the presence of a substantial population of (optically) obscured, luminous AGN at low redshifts, whose existence, instead, is suggested by *Chandra* results (see, e.g., Barger et al. 2001; Rosati et al. 2002). In our modeling we have not included any correction for type-II quasars, which appear to comprise between 30 per cent (La Franca et al. 2005), and ~ 80 per cent (Brown et al. 2005; Franceschini et al. 2005) of the quasar population at $0.5 < z < 2$. However, our model successfully reproduces the QSO LF in the hard X-ray band. Fig. 9 shows a comparison between the model predictions and the [2-10 keV] LF obtained by Ueda et al. (2003). The conversion from the hard-X band luminosity into a blue-band estimate has been done by assuming the scaling proposed by Marconi et al. (2004). We also compared the integrated mass density as a function of redshift to the redshift dependent integral of luminosity density of quasars (Marconi et al. 2004), including the X-ray LF (Ueda et al. 2003) and a correction of a factor 2 to account for missing Compton-thick quasars (Brown et al. 2005). We found a very good agreement over the whole redshift range probed by the LFs ($0 < z < 3$). We

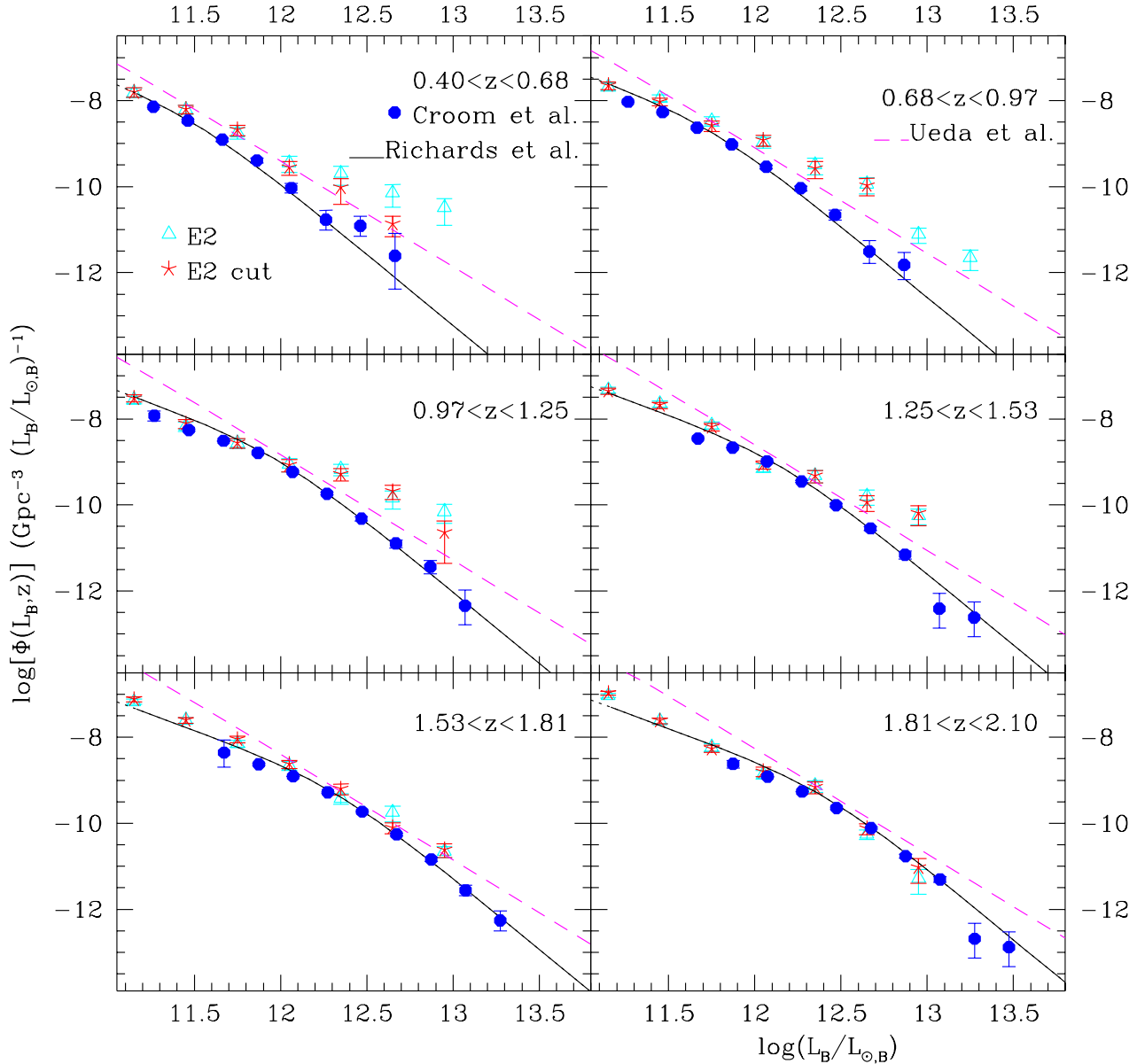


Figure 9. Comparison of the model predictions to the observed optical QSO LF (filled circles: C04; thin line: R05) and the hard X-ray LF (Ueda et al. 2003), converted into B -band (see text for more details). Symbols are as in Figs. 4 and 5.

therefore ascribe the discrepancy between model predictions and observations at optical wavelengths mainly to selection effects.

Second, Merloni et al. (2003) and Merloni (2004) have shown that low-redshift AGN are probably accreting inefficiently, i.e. both at an accretion rate much smaller than the Eddington rate and with a low radiative efficiency. Evidence for a BH powering mechanism less efficient at low redshift is also provided by the fact that local bright QSOs seem to be hosted in early-type galaxies that show no sign of recent merging events like disturbed morphology or recent star formation episodes (see, e.g., Grogin et al. 2005; Grazian et al. 2004; Dunlop et al. 2003, and references therein). These considerations suggest that a successful model for describing the evolution of QSO luminosity should include both a prescription for

a frequency-dependent galaxy obscuration and a more sophisticated mechanism for the QSO activity in which the BH accretion rate and the QSO duty-cycle might depend on halo masses and merger parameters, as suggested by recent numerical experiments (Di Matteo et al. 2005).

Both analytic and semi-analytic models predict a moderate degree of QSO clustering at low redshift, consistent with the observations. At higher redshifts ($z \approx 2$) the QSO biasing predicted by the analytic models appears to be significantly smaller than that of 2QZ/6QZ quasars. The only way for reproducing the observed degree of clustering is to increase the normalization constant ϵ in the $M_{\text{bh}} - v_c^2$ relation (Wyithe & Loeb 2005a), which, however, would overpredict the QSO number density in the local universe.

On the contrary, the redshift evolution predicted by semi-analytic schemes is significantly faster and matches observations out to $z \sim 2$. The high degree of clustering predicted by the semi-analytic VHM model does not derive from having placed the first seed BHs in correspondence of high- σ overdensity peaks of the mass density field. The adopted threshold, 3.5σ at $z = 20$, in fact corresponds to having at least one seed massive BH in haloes with $M_{\text{halo}} \simeq 10^{11} M_{\odot}$ at $z = 0$, which host massive BHs with masses well below that sampled by the optical LF of quasars. Moreover, dynamical effects such as the gravitational rocket (Volonteri & Perna 2005) can possibly eject BHs and thus lower the occupation fraction only in haloes with $M_{\text{halo}} < 10^{12} M_{\odot}$ that host BHs too faint to be included in the range probed by the optical LF. Placing seed BHs in correspondence of even higher peaks would certainly increase the biasing of the QSOs without modifying their luminosity function at $z > 0.5$, provided that the major merger threshold is changed accordingly (VHM). In this case, however, it would be difficult to explain the presence of SBHs in galaxies like the Milky Way or smaller, and, in general, AGN harboured in dwarf galaxies (Barth et al. 2005), which anyway are not sampled by the quasar LF at $z > 0.4$. The large values of bias in the semi-analytic models have a different explanation: it derives from the lack of a deterministic relation between the DM halo masses and the QSO luminosities at a given time. Indeed, a finite time is required to accrete a mass ΔM_{accr} to the central BH. During the accretion phase, the BH is smaller than predicted by the simple scaling relations with halo masses (i.e. $M_{\text{bh}} - \sigma_g$ or $M_{\text{bh}} - M_{\text{halo}}$). This means that, on average, the hosting halo of a quasar of a given luminosity is larger in the semi-analytic scheme than in the analytic models, the masses being the same only at the very end of the accretion episode. Consequently, the bias is enhanced in the semi-analytic model even if the LF looks similar.

In our analysis we have shown that simple models in which QSO activity is triggered by halo mergers within the framework of hierarchical build-up of cosmic structures can quantitatively describe the observed evolution of the quasar number counts and luminosity at all but very low redshifts, provided that some mechanisms are advocated to inhibit accretion within massive haloes hosting bright quasars. Semi-analytic schemes, that naturally account for the finite accretion time, are also capable of reproducing the observed QSO clustering at $z < 2$. These results suggest that the QSO evolution can probably be explained within the hierarchical scenario of structure formation in which the QSO activity mainly depends on the masses of their host haloes. More realistic models, however, should also account for the various halo properties including those of the baryons and for possible environmental effects. One possibility, which is most easily implemented within a semi-analytic scheme, is to include absorption effects and modify the accretion scheme accordingly using the outcomes of numerical hydrodynamical experiments. With this respect, we plan to modify the simple accretion scheme used in the VHM model following the recent results of Hopkins et al. (2005) who found that active QSOs are heavily obscured for most of their time but during their peak of activity when the surrounding dust is blown away and the QSOs shine prominently for a short period ($\sim 10^7$ yr).

It is worth stressing that the hierarchical models for QSO evolution and the possible modifications discussed so far rely on two important assumptions which have recently been cast into doubt. First of all, the models considered in this work assume a simple relation between QSO activity and the mass of its hosting halo. However, Wyithe & Loeb (2005b) pointed out that the tight relation between the BH mass and the velocity dispersion of the spheroid im-

plies that it is the spheroid rather than the halo which determines the growth of the SBHs and the subsequent QSO activity. As a consequence, the observed correlation between the halo and BH masses should not be regarded as fundamental as it merely reflects the fact that massive haloes preferentially host bulges with large velocity dispersions. This would imply that QSO activity, closely related to the evolution of bulges, should be studied using the more sophisticated models for galaxy formation and evolution. The second and more important issue is related to the results of the recent Millennium Simulation (Springel et al. 2005). The analyses performed by Gao et al. (2005) and by Harker et al. (2005) have shown that the spatial correlation properties and the formation epochs of the haloes depend on the local overdensity. This effect, which is particularly evident for galaxy-sized haloes, contradicts one of the basic assumption of the EPS theory which we have used to construct the halo merger history and to describe their biasing function. It is not clear, however, how serious the implications are for galaxy/QSO formation models and for halo models of clustering. In case they are and in absence of a generalized EPS theory capable of accounting for environmental effects (see, however, Abbas & Sheth 2005; Shen et al. 2005), then the only way out would be that of resorting to halo merger histories extracted from numerical experiments that implicitly account for environmental dependencies (see, e.g. Lemson & Kauffmann 1999). We will pursue this strategy in a subsequent work.

ACKNOWLEDGEMENTS

FM thanks the Institute of Astronomy, University of Cambridge, for the kind hospitality. MV acknowledges the warm and unforgettable hospitality at the Università degli Studi “Roma Tre”. We are grateful to Francesco Pace for useful discussions.

REFERENCES

- Abbas U., Sheth R. K., 2005, MNRAS, pp 986+
- Adelberger K. L., Steidel C. C., 2005, ApJ, 627, L1
- Barger A. J., Cowie L. L., Mushotzky R. F., Richards E. A., 2001, AJ, 121, 662
- Barkana R., Loeb A., 2001, Phys. Rep., 349, 125
- Barth A. J., Greene J. E., Ho L. C., 2005, ApJ, 619, L151
- Binney J., Tremaine S., 1987, Galactic dynamics. Princeton, NJ, Princeton University Press, 1987, 747 p.
- Bondi H., Hoyle F., 1944, MNRAS, 104, 273
- Brown M. J. I., et al., 2005, preprint, astro-ph/0510504
- Cattaneo A., 2001, MNRAS, 324, 128
- Cattaneo A., Blaizot J., Devriendt J., Guiderdoni B., 2005, MNRAS, 364, 407
- Cattaneo A., Haehnelt M. G., Rees M. J., 1999, MNRAS, 308, 77
- Cavaliere A., Vittorini V., 2000, ApJ, 543, 599
- Cavaliere A., Vittorini V., 2002, ApJ, 570, 114
- Cole S., Lacey C. G., Baugh C. M., Frenk C. S., 2000, MNRAS, 319, 168
- Croom S. M., et al., 2005, MNRAS, 356, 415
- Croom S. M., Smith R. J., Boyle B. J., Shanks T., Miller L., Outram P. J., Loaring N. S., 2004, MNRAS, 349, 1397
- Di Matteo T., Springel V., Hernquist L., 2005, Nat, 433, 604
- Dunlop J. S., McLure R. J., Kukula M. J., Baum S. A., O’Dea C. P., Hughes D. H., 2003, MNRAS, 340, 1095
- Efstathiou G., Rees M. J., 1988, MNRAS, 230, 5P

- Enoki M., Nagashima M., Gouda N., 2003, *pasj*, 55, 133
- Favata M., Hughes S. A., Holz D. E., 2004, *ApJ*, 607, L5
- Ferrarese L., 2002, *ApJ*, 578, 90
- Ferrarese L., Merritt D., 2000, *ApJ*, 539, L9
- Franceschini A., et al., 2005, *AJ*, 129, 2074
- Gao L., Springel V., White S. D. M., 2005, *MNRAS*, 363, L66
- Gebhardt K., et al., 2000, *ApJ*, 539, L13
- Grazian A., Negrello M., Moscardini L., Cristiani S., Haehnelt M. G., Matarrese S., Omizzolo A., Vanzella E., 2004, *AJ*, 127, 592
- Grogin N. A., et al., 2005, *ApJ*, 627, L97
- Haehnelt M. G., Rees M. J., 1993, *MNRAS*, 263, 168
- Haiman Z., Loeb A., 1998, *ApJ*, 503, 505
- Haiman Z., Menou K., 2000, *ApJ*, 531, 42
- Harker G., Cole S., Helly J., Frenk C., Jenkins A., 2005, preprint, astro-ph/0510488
- Hatziminaoglou E., Mathez G., Solanes J.-M., Manrique A., Salvador-Solé E., 2003, *MNRAS*, 343, 692
- Hatziminaoglou E., Siemiginowska A., Elvis M., 2001, *ApJ*, 547, 90
- Hopkins P. F., Hernquist L., Martini P., Cox T. J., Robertson B., Di Matteo T., Springel V., 2005, *ApJ*, 625, L71
- Kauffmann G., Haehnelt M., 2000, *MNRAS*, 311, 576
- La Franca F., et al., 2005, preprint, astro-ph/0509081
- Lacey C., Cole S., 1993, *MNRAS*, 262, 627
- Lemson G., Kauffmann G., 1999, *MNRAS*, 302, 111
- Madau P., Rees M. J., Volonteri M., Haardt F., Oh S. P., 2004, *ApJ*, 604, 484
- Magorrian J., et al., 1998, *AJ*, 115, 2285
- Marconi A., Risaliti G., Gilli R., Hunt L. K., Maiolino R., Salvati M., 2004, *MNRAS*, 351, 169
- Martini P., Weinberg D. H., 2001, *ApJ*, 547, 12
- Merloni A., 2004, *MNRAS*, 353, 1035
- Merloni A., Heinz S., di Matteo T., 2003, *MNRAS*, 345, 1057
- Merritt D., Milosavljević M., Favata M., Hughes S. A., Holz D. E., 2004, *ApJ*, 607, L9
- Milosavljević M., Merritt D., 2001, *ApJ*, 563, 34
- Mo H. J., White S. D. M., 1996, *MNRAS*, 282, 347
- Page M. J., Carrera F. J., 2000, *MNRAS*, 311, 433
- Peacock J. A., Dodds S. J., 1996, *MNRAS*, 280, L19
- Percival W., Miller L., 1999, *MNRAS*, 309, 823
- Peters P. C., 1964, *Physical Review*, 136, 1224
- Porciani C., Magliocchetti M., Norberg P., 2004, *MNRAS*, 355, 1010
- Quinlan G. D., 1996, *New Astronomy*, 1, 35
- Richards G. T., et al., 2005, *MNRAS*, 360, 839
- Richstone D., et al., 1998, *Nat*, 395, A14+
- Rosati P., et al., 2002, *ApJ*, 566, 667
- Shen J., Abel T., Mo H., Sheth R., 2005, preprint, astro-ph/0511365
- Sheth R. K., Tormen G., 1999, *MNRAS*, 308, 119
- Silk J., Rees M. J., 1998, *A&A*, 331, L1
- Somerville R. S., Kolatt T. S., 1999, *MNRAS*, 305, 1
- Springel V., Di Matteo T., Hernquist L., 2005, *MNRAS*, 361, 776
- Springel V., et al., 2005, *Nat*, 435, 629
- Steidel C. C., Hunt M. P., Shapley A. E., Adelberger K. L., Pettini M., Dickinson M., Giavalisco M., 2002, *ApJ*, 576, 653
- Tremaine S., et al., 2002, *ApJ*, 574, 740
- Ueda Y., Akiyama M., Ohta K., Miyaji T., 2003, *ApJ*, 598, 886
- Volonteri M., Haardt F., Madau P., 2003, *ApJ*, 582, 559
- Volonteri M., Madau P., Haardt F., 2003, *ApJ*, 593, 661
- Volonteri M., Perna R., 2005, *MNRAS*, 358, 913
- Volonteri M., Rees M. J., 2005, *ApJ*, 633, 624
- Wyithe J. S. B., Loeb A., 2002, *ApJ*, 581, 886
- Wyithe J. S. B., Loeb A., 2003, *ApJ*, 595, 614
- Wyithe J. S. B., Loeb A., 2005a, *ApJ*, 621, 95
- Wyithe S., Loeb A., 2005b, preprint, astro-ph/0506294